Droplet-on-demand printing of polymer solutions

J. Frits Dijksman[1] and Paul C. Duineveld [2]

[1] Physics of Fluids (Chair Innovative Biomedical Applications of Inkjet Technology), Faculty Science and Technology, University of Twente, Enschede, The Netherlands

[2] Philips Consumer Lifestyle Technology Expert Group, Drachten, The Netherlands

Abstract

Droplet-on-demand inkjet printing of polymer solutions offers the possibility to deposit in a patterned way very small amounts of polymer functional materials. One of the characteristics of jetting on demand polymer solutions is the existence of a long stretching fluid filament between the main droplet and the fluid contained in the nozzle. The forces generated in the stretching fluid filament may be so large that initially the droplet leaves the nozzle but is retracted in course of its flight. The very existence of the fluid filament is a sign of the viscoelastic nature of the ink used. By investigating carefully the kinematics and dynamics involved in the stretching of the fluid filament, the rheology of the ink can be retrieved, especially its elongational properties. The kinematics involves the stretching of the fluid filament, the growth of the droplet during flight and tail hooking. The dynamics involve the deceleration of the main droplet, viscous forces and surface tension.

Introduction

Droplet-on-demand inkjet printing of polymer solutions offers the possibility to deposit in a patterned way very small amounts of polymer functional materials. Examples of applications are biosensors [1,2] (printing DNA capture molecules dissolved in a buffer), manufacturing of displays [3] (depositing of polymer light emitting materials dissolved in an organic solvent), manufacturing of IC's using the concepts of directed self-assembly [4] (solution processing of PMMA-PS block copolymers) and nano-imprint technology [5,6] (patterning of photosensitive resist). One of the characteristics of jetting on demand polymer solutions is the existence of a long stretching fluid filament between the main droplet and the fluid contained in the nozzle [7,8,9]. The forces generated in the stretching fluid filament may be so large that initially the droplet leaves the nozzle but is retracted in course of its flight. The very existence of the fluid filament is a sign of the viscoelastic nature of the ink used. By investigating carefully the kinematics and dynamics involved in the stretching of the fluid filament, the rheology of the ink can be retrieved, especially its elongational properties. The kinematics involves the stretching of the fluid filament, the growth of the droplet during flight, and tail hooking. The dynamics is about the deceleration of the main droplet, viscous forces and surface tension.

The starting point of the analysis is a series of images displaying the droplet formation of a viscoelastic ink in course of time. The pitch of the nozzles is used to calculate real dimensions.
The kinematics of the stretching fluid filament contains two distinct features: the elongation of the fluid filament and the wave speed of the tail hook. The dynamics are controlled by Newton's law, by measuring the deceleration and growth of the droplet, viscous forces and surface tension. Elongation and the travelling tail hook are related to uniaxial stretching. From these phenomena the elongational viscosity can be derived, defined as the ratio of the elongational stress and the rate of elongation. Elastic effects are assumed to have reached an equilibrium state (already most probably in the nozzle).
A measure for the non-Newtonian behavior of the fluid is the Trouton ratio, the ratio of the elongational viscosity and the shear viscosity. Apart from the material used this ratio is also dependent on the flow field. For a Newtonian liquid loaded in uniaxial tension the Trouton ratio is equal to 3 (for planar extension 4). For the ink investigated in this paper this value appears to be 4 times as high in uniaxial stretching.

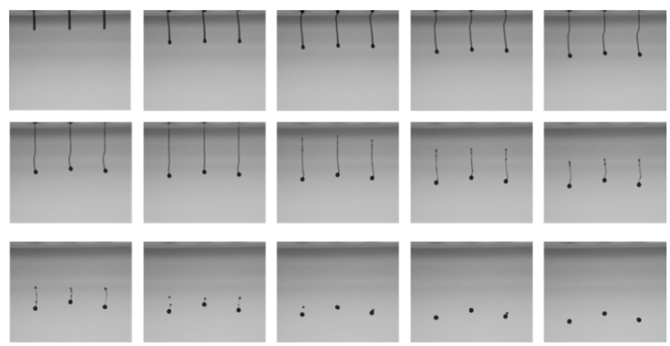

Figure 1 Series of photographs showing the evolution of the droplet formation of a viscoelastic ink. The pitch between nozzles is 254 µm, the timing starts at 10 µs after the leading edge of the pulse, followed by images 10 µs apart in course of time. Tail hooking starts at the second image, there the tip of the tail in the nozzle is displaced to the left, in the third image the tail is centered again and a wave crest starts to travel downwards.

Experiments

The jetting experiments have been carried out with a Dimatix 256 nozzle Galaxy print head with 30 micron nozzles [10]. The fluid was a solution of a light emitting polymer in anisole (≈1% by weight, no further details available due to confidentiality). The flow properties of anisole at ambient conditions (1 bar and 20 °C) are:

- viscosity μ = 1.05 mPas,
- surface tension γ = 30 mN/m and
- density ρ = 953 kg/m^3

The maximum amount of polymer was chosen such that shear viscosity of the solution was tuned to as low as 10 mPa.s, a value prescribed by the print head manufacturer. The shear viscosity has

a Newtonian plateau and shows some shear thinning at high shear rates (>10^4 1/s). The relaxation time is about 0.1 ms. The added polymer has no influence on the density and surface tension.
The images were obtained by stroboscopic illumination of the droplet formation. The stroboscope was triggered by the leading edge of the electrical pulse to the print head (all nozzles are fired at the same time). The pulse length of the stroboscope was about 1 µs. By varying the time delay between the leading edge and the stroboscope droplet formation is recorded at different time instances. As the droplet formation is extremely stable concatenating of these images delivers a "high speed" movie of the droplet formation. It should be noted that fine details of the droplet formation such as the occurrence of small satellite droplets, do show unrealistic temporal behavior due to the fact that the images are made over time, each image showing one individual droplet at a specific delay. The pitch of the nozzles of the Dimatix Galaxy head is 254 µm.

Results of measurements

From the series of images the droplet position and growth can be obtained and also the volume of the tail, see figures 2 and 3.

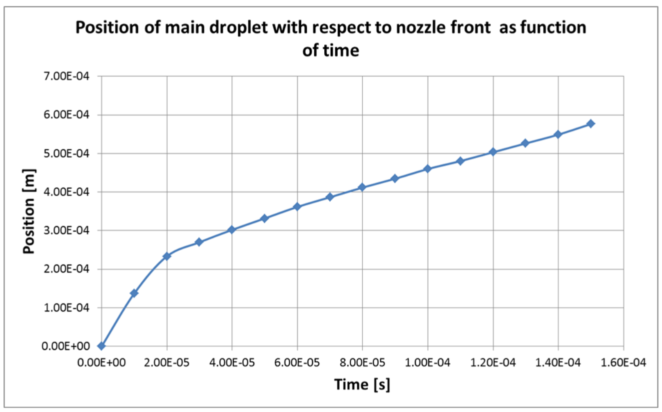

Figure 2 Measured droplet position (centre of gravity) as function of time (this result has been used for the tail length as long as the fluid filament is connected to the fluid in the nozzle).

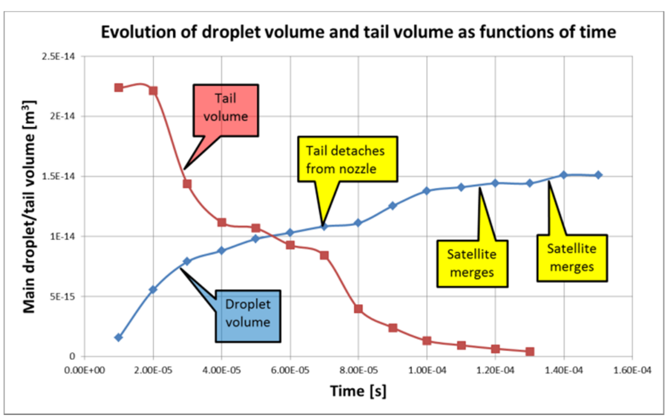

Figure 3 Measured droplet and tail volume as functions of time. The blue line(diamonds) shows the volume of the droplet, the red line (squares) the tail volume. In yellow characteristic phenomena are indicated such as the time instant at which the tail detaches from the nozzle and the two moments in time where a satellite droplet merges with the main droplet (see figure 1 for details).
The error in measuring the volume of the droplet is about 1 - 2 pl (1 pl = 10^{-15} m^3). The error in measuring the tail volume is somewhat larger, especially when the tail becomes very thin.

The tail shows a wave travelling downwards. The speed of the crest of the wave is depicted in figure 4. This effect is often referred to as tail hooking [11,12]. It is caused by a fluidic instability in the nozzle. At a certain moment the meniscus is retracted inside the nozzle while the tail is still connected to the fluid contained in the nozzle, causing the tail to slip to the edge of the nozzle. A short while later the fluid moves outside the nozzle and the tail moves back to the centerline. The motion of the fluid in the nozzle is directly correlated to the internal acoustics of the print head.

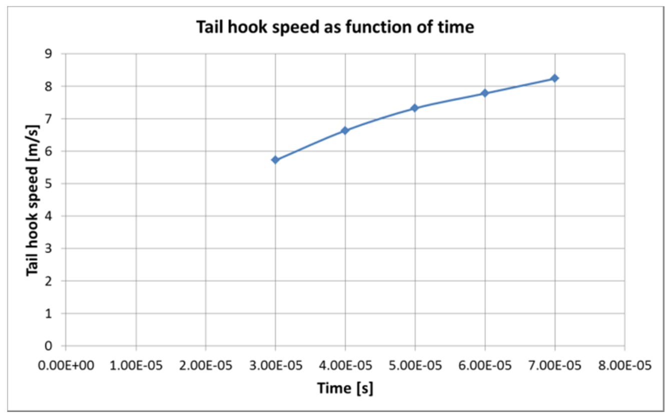

Figure 4 Speed of the crest of the wave travelling downwards along the filament.

The initial droplet plus tail volume equals 28 pl, the final droplet volume amounts to 15 pl.

Analysis

Elongational viscosity

Starting from the position of the center of gravity of the droplet as a function of time the velocity of the droplet and also the deceleration can be obtained. For the case shown in figure 1, the velocity of the center of gravity of the main droplet goes from initially 12 m/s down to 2.5 m/s and gradually approaches 2 m/s. The deceleration is almost a constant after the initial phase and equals 2 x 10^4 m/s^2. By differentiation oscillations in velocity and acceleration become visible. These oscillations can be attributed to the internal acoustics of the print head. As shown in figure 3 the volume of the droplet grows in course of time, consuming part of the tail volume for this particular setting of the driving of the print head. Accordingly the tail volume decreases. The tail volume decreases faster than the droplet grows, indicating that some fluid is pushed back into the nozzle.
The kinematics of the droplet formation is controlled by the fluid delivered through the nozzle, the tail formation and the growth of

the droplet; the dynamics by the stretching fluid filament, surface tension and momentum transport. Surface tension effects are given by (sum of surface tension along the circumference of the filament and the normal stress induced by the pressure inside the filament generated by the very same surface tension, γ surface tension and $R_{jet}(t)$ the temporal radius of the filament):

$$F_{surface\ tension}(t) = 2\gamma\pi R_{jet}(t) - \gamma\pi R_{jet}(t) = \gamma\pi R_{jet}(t) \quad (1)$$

To stretch the filament a viscous force is needed of which the value is given by (μ shear viscosity and $\dot{\varepsilon}(t)$ the rate of elongational):

$$F_{elongation}(t) = 3K\mu\dot{\varepsilon}(t)\pi R_{jet}^2(t) \quad (2)$$

$$\dot{\varepsilon}(t) = (v_d(t) + 2v_e(t))/l_{filament}(t) \quad (3)$$

The draining velocity v_e is given by the ratio of the rate of change of the droplet volume and the momentary cross-section. Note that v_e is defined with respect to the moving droplet:

$$v_e = \frac{dV_{droplet}}{dt}/(\pi R_{jet}{}^2) \quad (4)$$

The factor 3 in (2) is often referred to as the Trouton ratio [13]. This value only holds true for Newtonian liquids. Measured deviations from this value will be considered a sign of non-Newtonian behavior and are incorporated into the factor K, the larger K the more non-Newtonian the liquid will be. In (3) the elongational rate depends on the droplet velocity giving the rate of change of the length of the filament and the draining velocity v_e, related to the gain of volume of the droplet. Here it is assumed that what happens at the droplet end of the filament will happen at the nozzle side as well. This assumption is confirmed by the fact that in the end about half of the initial filament volume ends up in the droplet. The other half is delivered back to the fluid contained in the nozzle.

We now consider the dynamics of the droplet. The surface tension force and the elongational force direct upwards decelerating the droplet. As the filament empties itself into the droplet momentum is transferred to droplet, similar as for a rocket. A rocket is accelerated by the thrust of the engine and by losing at the same time its weight. For our case the thrust comes from the fluid flowing into the droplet and by the gain in weight. This means that this effect accelerates the droplet (q mass flow rate):

$$F_{propulsion} = qv_e \qquad q = \rho\frac{dV_{droplet}}{dt} \quad (5)$$

The equation of motion of the droplet reads:

$$F = ma = F_{propulsion} - F_{elongation} - F_{surface\ tension} \quad (6)$$

The acceleration term a equals -2*10^4 m/s^2, m is momentary mass of the droplet. From equation (6) the elongational force and finally the factor K can be derived:

$$K = \frac{F_{propulsion} - F_{surface\ tension} - ma}{3\mu\dot{\varepsilon}\pi R_{jet}^2} \quad (7)$$

The result is given in figure 5. Here we have combined the results of two measurements: one at a low droplet velocity (2 m/s) and a second with a high droplet velocity (5 m/s). Consistently, $K > 1$, roughly equal to 4, indicating that the liquid used is non-Newtonian. The scatter in the data is due to the fact that small errors in the determination of position of the droplet and the radius of the filament are enlarged (acceleration needs two times differentiation, errors in the radius are enlarged twofold as we need the cross-section rather than the radius itself).

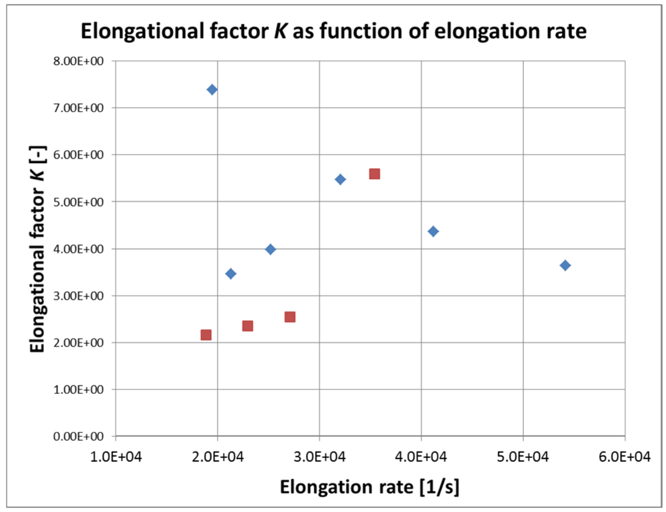

Figure 5 Elongational factor K as function of elongational rate (red squares apply for a 2 m/s droplet velocity case, the blue diamonds for a 5 m/s droplet velocity case).

Wave speed as force "transducer"

Another effect we want to deal with is the speed of the crest of the wave travelling downwards along the filament [14]. The equation of motion of an infinitesimal small portion δx of a string with cross section A and density ρ under tension T is given by (x co-ordinate along the string and y the displacement):

$$\rho A\delta x\frac{\partial^2 y}{\partial t^2} = T\frac{\partial^2 y}{\partial x^2}\delta x \quad (8)$$

The wave speed of a disturbance along the string reads:

$$v = \sqrt{\frac{T}{\rho A}}, \quad T = v^2\rho A \quad (9)$$

That means that by measuring the wave speed the tension force in the spring can be determined. We see so to say the tension. In our case we have to deal with a string of which the cross section changes over time:

$$\frac{\partial}{\partial t}\rho\pi R_{jet}{}^2\delta x\frac{\partial y}{\partial t} = T\frac{\partial^2 y}{\partial x^2}\delta x$$
$$\rho\pi R_{jet}{}^2\frac{\partial^2 y}{\partial t^2} + \rho\pi 2R_{jet}\frac{dR_{jet}}{dt}\frac{\partial y}{\partial t} = T\frac{\partial^2 y}{\partial x^2} \quad (10)$$

When considering the travelling of a local disturbance almost everywhere y is zero and (10) is fulfilled all the time. The timing of tail hooking, being an left/right event, measures $\tau = 1/(2f)$ and is driven by the internal acoustics of the print head (f = 50-60 kHz). The length scale of the disturbance caused by tail hooking is $v\tau/2$ (within τ the disturbance moves to the left and back again to the center). The equation (9) is scaled using the following the scaling:

$$t = \tau t^*, \quad x = \frac{v\tau}{2} x^* \tag{10}$$

Upon substitution we get:

$$\frac{\rho \pi {R_{jet}}^2}{\tau^2} \frac{\partial^2 y}{\partial t^{*2}} + \frac{\rho \pi 2 R_{jet}}{\tau} \frac{dR_{jet}}{dt} \frac{\partial y}{\partial t^*} = \frac{4T}{v^2 \tau^2} \frac{\partial^2 y}{\partial x^{*2}} \tag{11}$$

All terms involving y are now of equal magnitude and the time dependent tension T is given by:

$$T = \frac{1}{4} v^2 \rho \pi {R_{jet}}^2 \left(1 + 2\tau \frac{1}{R_{jet}} \frac{dR_{jet}}{dt} \right) \tag{12}$$

Given the time evolution of the radius of the filament, the speed of the crest of the wave travelling downwards along the filament and the characteristic time of the print head τ (of which the value depends on the internal acoustics of the print head) the tension in the filament can be calculated as a function of time. This value should be equal to the deceleration force acting on the droplet. Using again the time series of images of figure 1 the result is shown in figure 6.

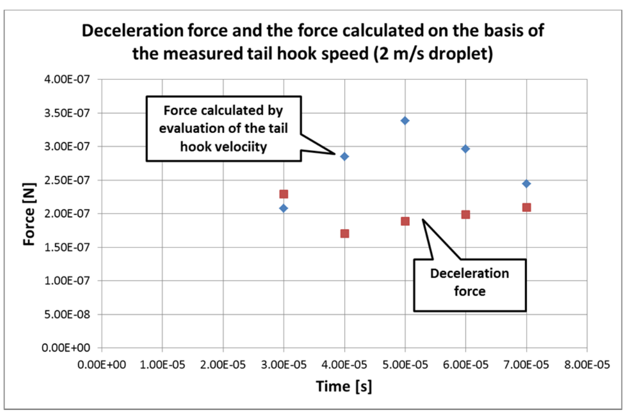

Figure 6 Deceleration force acting on droplet (shown positive) and the tension force calculated using (12). The internal key note frequency of the print head in taken equal to 50 kHz.

The correspondence between the force calculated by considering the deceleration of the growing droplet on the one hand and the force calculated using the information coming from the speed of the wave crest travelling downwards along the filament and internal acoustics of the print head on the other hand is good as far as the order of magnitude is concerned. Again we have to stress that this result especially for the tension is hampered by the amplification of small errors.

Concluding remarks

We have shown that by observing carefully the evolution of the droplet size and the filament characteristics such as cross section and length can be used to measure the elongational characteristics of non-Newtonian inks at elongation rates hardly accessible by standard rheometers. As the volume of the filament decreases in course of time, the elongation rate of the filament is much higher than the value obtained by just using the ratio of the momentary droplet velocity and filament length.
An interesting extra feature is that tail hooking can be used as a kind of force “transducer”, the observed wave speed contains direct information about the tension in the filament. Therefore it is needed to solve the wave equation for a stretching filament.

References

[1] Anke Pierik, Marius Boamfa, Martijn van Zelst, Danielle Clout, Henk Stapert, Frits Dijksman, Dirk Broer and Reinhold Wimberger-Friedl, “Real time quantitative amplification detection on a microarray: towards high multiplex quantitative PCR”, *Lab Chip*, **2012**, 12, 1897

[2] J. Frits Dijksman, Anke Pierik, “Fluid dynamical analysis of the distribution of ink jet printed biomolecules in microarray substrates for genotyping applications”, *BIOMICROFLUIDICS* 2, 044101 (**2008**)

[3] J. F. Dijksman, P. C. Duineveld, M. J. J. Hack, A. Pierik, J. Rensen, J.-E. Rubingh, I. Schram and M. M. Vernhout, “Precision ink jet printing of polymer light emitting displays”, *J. Mater. Chem*., **2007**, 17, 511–522

[4] S.F. Sander, D. Ambesi, T.S. Druzhinina, E. Peeters, J. Finders, J. Klein Wolterink and J.G. E. M. Fraaije, “Fundamental study of placement errors in directed self-assembly”, *J. Micro/Nanolith. MEMS MOEMS* 033005-1-8 Jul–Sep **2014**, Vol. 13(3)

[5] S.F. Wuister, J.H. Lammers, Y.W. Kruijt-Stegeman and J.F. Dijksman J, “Squeeze time investigations for step and flash imprint lithography”, *MICROELECTRONIC ENGINEERING* Volume: 86 Issue: 4-6 Pages: 681-683 (**2009**)

[6] I. Reinhold, M.S. Shafran, W. Longsine, M.c. Traub, Y. Srinivasan, V.N. Truskett and W. Zapka, “High-Speed, Low-Volume Inkjet and its Role in Jet and Flash Imprint Lithography”, *NIP* **2014**, Philadephia.

[7] P.C. Duineveld, J.F. Dijksman, H. Huang, “Non-Newtonian effects of ink-jet printed droplets”, *XXI International Congress of Theoretical and Applied Mechanics*, Warsaw, Poland, August 15-21, **2004**

[8] Stephen D. Hoath, Oliver G. Harlen and Ian M. Hutchings, “Jetting behavior of polymer solutions in drop-on-demand inkjet printing”, *J. Rheol.* 56(5), 1109-1127 (**2012**)

[9] Sungjune Jung, Stephen D. Hoath and Ian M. Hutchings, “The role of viscoelasticity in drop impact and spreading for inkjet printing of polymer solution on a wettable surface”, *Microfluid Nanofluid* (**2013**) 14:163–169

[10] www.fujifilmusa.com

[11] O.G. Harlen, J.R. Castrejon-Pita, A. Castrejon-Pita, “Asymmetric Detachment from Angled Nozzle Plates in Drop on Demand Inkjet Printing”, NIP & Digital Manufacturing Conference 2013, pp 277-280.

[12] M.P. van der Meulen, “Meniscus Motion and Drop Formation in Inkjet Printing”, Thesis University of Twente, February 19-th, 2015.

[13] R.B. Bird, R.C. Armstrong and O. Hassager, “Dynamics of Polymeric Liquids”, Second Edition, Volume 1, John Wiley & Sons, 1987, pp 38-39.

[14] G.C. King, “Vibrations and Waves”, Jon Wiley & Sons, 2009, chapter 5

Authors Biographies

J. Frits Dijksman *obtained his masters in mechanical engineering at the Technical University of Delft in The Netherlands in 1973. He finished his PhD within the groups of Professor. D. de Jong and Professor W.T. Koiter (Technical University of Delft, The Netherlands, 1978) focussing on the engineering mechanics of leaf spring mechanisms. He worked with Philips Research Laboratories in Eindhoven, The Netherlands for 32.5 years. After his retirement he continued his work as part time professor at the University of Twente, The Netherlands. The topics include inkjet printing of viscoelastic inks, design of inkjet print heads and printed biosensors.*

Paul C. Duineveld *graduated and did his PhD at Twente University under supervision of Leen van Wijngaarden on bubble dynamics. After his service as Navy officer he started at Philips Research working, together with Frits Dijksman, mainly on inkjet printing for display and bio-sensor applications. In 2004 he moved to Philips Consumer Lifestyle where he started working on what is now Philips AirFloss. In 2007 he became a director of Engineering in the field of Fluid Dynamics and in 2008 a DFSS BB. He is the principal in a team of 7 people working on fluid dynamic applications in household appliances from vacuum cleaners, irons, air purifiers, baby bottles, toothbrushes, fruit juicers, coffeemakers etc.*